ACS OMEGA

http://pubs.acs.org/journal/acsodf

Article

Development of Gelatin-Based Shape-Memory Polymer Scaffolds with Fast Responsive Performance and Enhanced Mechanical Properties for Tissue Engineering Applications

Na Eun Kim, Sunjae Park, Sooin Kim, Joo Hee Choi, Se Eun Kim, Seung Ho Choe, Tae woong Kang, Jeong Eun Song, and Gilson Khang*

Cite This: *ACS Omega* 2023, 8, 6455−6462

Read Online

ACCESS | Metrics & More | Article Recommendations

ABSTRACT: Shape-memory polymers (SMPs) can be defined as a reversibly changing form through deformation and recovery by external stimuli. However, there remain application limitations of SMPs, such as complicated preparation processes and slow shape recovery. Here, we designed gelatin-based shape-memory scaffolds by a facile dipping method in tannic acid solution. The shape-memory effect of scaffolds was attributed to the hydrogen bond between gelatin and tannic acid, which acts as the net point. Moreover, gelatin (Gel)/oxidized gellan gum (OGG)/calcium chloride (Ca) was intended to induce faster and more stable shape-memory behavior through the introduction of a Schiff base reaction. The chemical, morphological, physicochemical, and mechanical properties of the fabricated scaffolds were evaluated, and those results showed that the Gel/OGG/Ca had improved mechanical properties and structural stability compared with other scaffold groups. Additionally, Gel/OGG/Ca exhibited excellent shape-recovery behavior of 95.8% at 37 °C. As a consequence, the proposed scaffolds can be fixed to the temporary shape at 25 °C in just 1 s and recovered to the original shape at 37 °C within 30 s, implying a great potential for minimally invasive implantation.

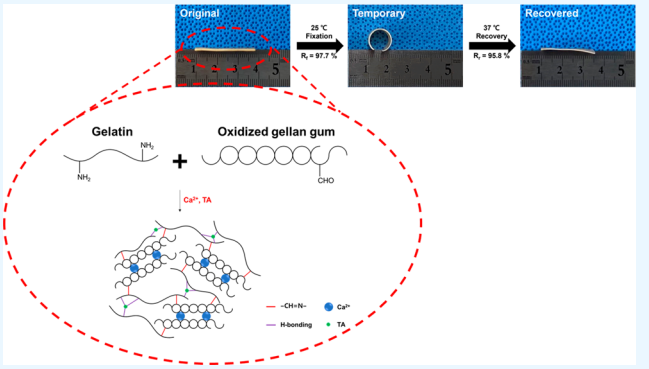

INTRODUCTION

Shape-memory polymers (SMPs) can be defined as a reversibly changing form through deformation and recovery by external stimuli such as temperature, pH, electric fields, light, and chemicals.[1,2] By applying proper stimulation to the materials, SMPs have a permanent shape and a temporary shape. Because they have this differentiation from other polymers, they are spotlighted as an effective polymer in biomedical fields such as minimally invasive surgery[3,4] and sutures.[5]

Among the various stimuli for transformation, there are many previous studies about thermally induced SMPs being used for scaffold production in tissue engineering.[6−9] Materials such as polytetrafluoroethylene (PFTE), polylactide (PLA), and polyvinyl acetate ethylene (EVA) have been suggested as thermally induced SMPs.[10−12] These materials have a specific temperature called a transition temperature (T_{trans}), which changes from a permanent shape to a temporary shape. However, since most T_{trans} of these materials exceed the physiologically active temperature, it causes problems in applications to the human body.[6,13,14] In addition, not only is the process complicated, but there remains a challenge that takes a long time to change the shape.[3,15]

Herein, we propose temperature response SMPs prepared from gelatin with an easier process and faster shape recovery than previous studies. Gelatin is an appropriate material because it has the ability to form good film formation and biocompatibility.[16,17] In addition, more importantly, it has a reversible triple helix structure through the temperature change and forms a cross-linked molecular chain structure at low temperatures.[18−20] Although it has properties suitable for SMPs, gelatin has limitations because of its weak mechanical properties and rapid degradation.[21] Since the scaffold must have appropriate mechanical properties in terms of tissue engineering,[22] tannic acid and oxidized gellan gum (OGG) were used to increase the mechanical strength through various chemical bonds.[23,24] Tannic acid can have a strong interaction with gelatin through hydrogen bonding,[25] and oxidized gellan

Received: October 19, 2022
Accepted: January 31, 2023
Published: February 10, 2023

https://doi.org/10.1021/acsomega.2c06730
ACS Omega 2023, 8, 6455−6462

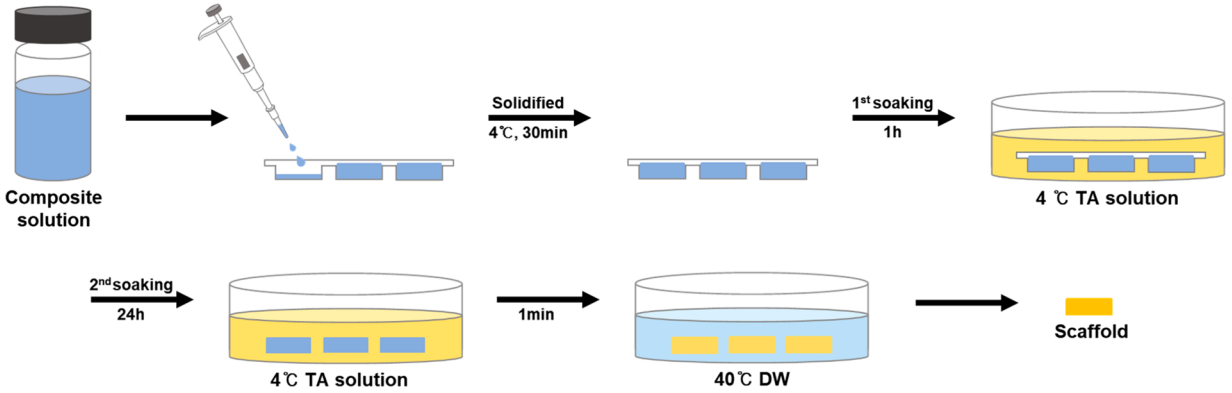

Figure 1. Schematic illustration of the preparation of gelatin-based scaffolds.

gum can have physical cross-linking by blending with a small amount of calcium chloride ($CaCl_2$).

To demonstrate these novel SMPs, the morphological, physicochemical, and mechanical properties were evaluated by Fourier transform infrared spectroscopy (FT-IR), field emission scanning electron microscopy (FE-SEM), mass swelling, sol fraction, weight loss, porosity, and tensile test. Also, an in vitro study with a cytotoxicity test was performed.

EXPERIMENTAL SECTION

Preparation of Oxidized Gellan Gum. The oxidized gellan gum was fabricated according to a method reported in a previous study.[26] First, 1% (w/v) gellan gum (GG) (Gelzan, Sigma-Aldrich, USA) was added into distilled water (DW) and stirred at 90 °C until completely dissolved. Then after the solution was cooled to 40 °C, 0.25 M sodium periodate ($NaIO_4$), an oxidizing agent, was added in a dropwise manner for 90 min. Ethylene glycol (Sigma-Aldrich, USA) was added to the solution and stirred for 30 min to stop the oxidation reaction. The mixture was dialyzed with 14,000 (14k) molecular weight cutoff membranes for 3 days in DW to remove the excess $NaIO_4$ and ethylene glycol. After that, the product was freeze-dried for 7 days and stored in a desiccator.

Preparation of Gel, Gel/Ca, and Gel/OGG/Ca Scaffolds. The scaffolds were prepared by slightly modifying the previous study.[27] The scaffolds were prepared by dipping the scaffolds made of three different mixtures in TA (Sigma-Aldrich, USA) solution (Figure 1). All groups were fabricated by blending gelatin solution with other materials. 1% (w/v) OGG was stirred in DW at 90 °C until it was homogeneously dissolved. The OGG solution was cooled to 60 °C, and 10% (w/v) gelatin (gel, type A from porcine skin, Sigma-Aldrich, USA) was added and stirred for 1 h to fully dissolve. Then $CaCl_2$ (Ca, SHOWA, Japan) was added to make a composite solution of 10% Gel, 1% OGG, and 0.5% (w/v) Ca (Gel/OGG/Ca). Then gelatin was stirred in DW at 60 °C to make a 10% (w/v) gelatin solution. $CaCl_2$ was added to a prepared gelatin solution to obtain a composite solution of 10% Gel and 0.5% (w/v) Ca (Gel/Ca). Each composite solution was rapidly poured into laboratory-made silicon molds that were preheated at 60 °C to obtain a uniformly dispersed solution. The prepared specimens were stored at 4 °C for 30 min to solidify. The solidified samples were immersed in TA solution in two steps. First, the molds with samples were immersed in 1% (w/v) TA solution at 4 °C for 1 h (the first soaking). In the second step, the molds were removed and the samples were immersed in 1% (w/v) TA solution at 4 °C for 24 h (the second soaking). Finally, the scaffolds were immersed in DW at 40 °C for 1 min.

Chemical Structure Analysis. The chemical structures of the samples were analyzed by FT-IR (PerkinElmer, USA) spectroscopy in the wavelength range of 400−4000 cm^{-1}. All of the samples were freeze-dried for measurement.

Morphological Observation. The surface morphology of the samples was obtained by FE-SEM (Carl Zeiss, Germany). The samples were lyophilized and coated with platinum for observation.

Mass Swelling. The prepared samples were placed in a 24-well plate and then stored in a 37 °C incubator for 24 h after phosphate-buffered saline (PBS, Gibco, USA) was added. After removing PBS, the weight was measured (W_w) and the mixture subsequently lyophilized for 48 h. The weight of these lyophilized samples was measured (W_l). The swelling ratio was calculated using eq 1:

$$\text{mass swelling} = \frac{W_w}{W_l} \tag{1}$$

Sol Fraction. The sol fraction was evaluated by measuring the initial weight of the lyophilized samples (m_i). Then the measured samples were immersed in DW and agitated on a shaker for 1 h at 60 rpm. The hydrated samples were freeze-dried again and weighed (m_f). The sol fraction was calculated using eq 2:

$$\text{sol fraction (\%)} = \frac{m_i - m_f}{m_f} \times 100\ (\%) \tag{2}$$

Weight Loss. The initial weight of the freeze-dried samples was measured (W_i) and placed in PBS at 37 °C. PBS was removed, and the samples were rinsed with DW three times and freeze-dried. The weight of the freeze-dried samples was measured (W_f). The weight loss was calculated using eq 3:

$$\text{weight loss (\%)} = \frac{W_i - W_f}{W_i} \times 100\ (\%) \tag{3}$$

Porosity. The porosity of the samples was evaluated by the principle of Archimedes via the fluid displacement measurement technique. Before the analysis, the length and height of the test sample were measured. Then samples were immersed in PBS and stored in a 37 °C incubator for 24 h. The hydrated samples were removed, and the remaining volume of PBS was measured as V_3. The first amount of PBS is referred to as V_1, and the value of adding the volume of samples to V_1 is referred to as V_2. Porosity was calculated using eq 4:

https://doi.org/10.1021/acsomega.2c06730
ACS Omega 2023, 8, 6455−6462

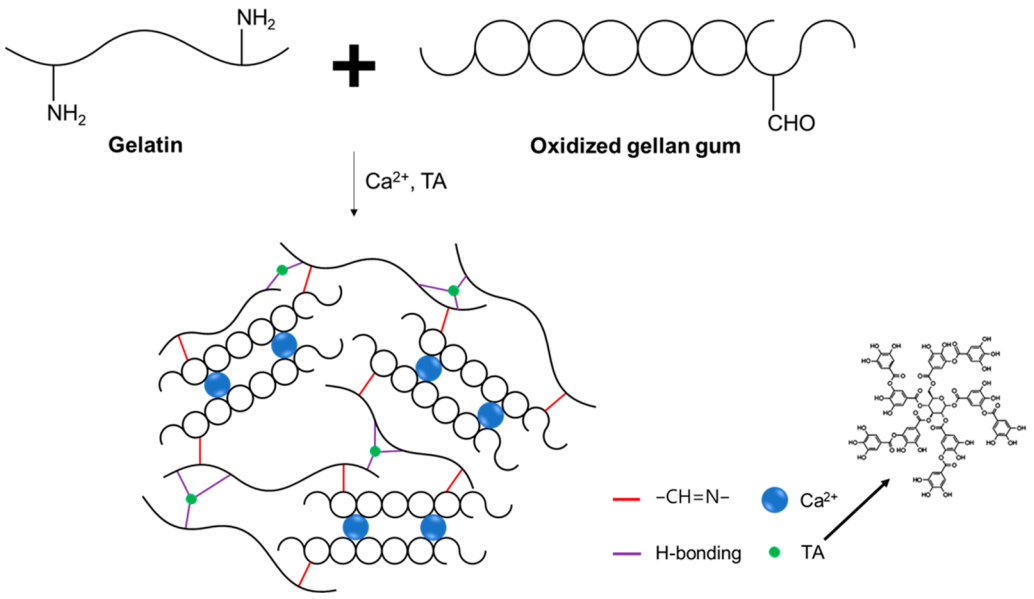

Figure 2. Schematic illustration of Gel/OGG/Ca scaffold synthesis.

$$\text{porosity}\ (\%) = \frac{V_1 - V_3}{V_2 - V_3} \times 100\ (\%) \tag{4}$$

Mechanical Measurements. The tensile tests were evaluated using a universal testing machine (UTM, Galdabini, Italy). All of the samples were prepared at a length of 40 mm, a width of 11 mm, and a thickness of 0.5 mm and tested immediately after fabrication to prevent moisture evaporation. Tensile tests were performed at a speed of 20 mm/min until the specimen was fractured.

Shape-Memory Behavior. To observe the temperature-responsive shape-memory behavior, all of the samples were cut into a length of 30 mm and a width of 10 mm and treated in 40 °C DW for 1 min. The sample was dipped in 37 °C DW for 1 s. Then the sample was taken out, and the shape was softly altered by wrapping on a glass rod. Next, the transformed sample was dipped in 25 °C DW for 1 s to fix the shape. The shape-recovery process from the transformed shape to the original shape was triggered by immersing samples into the 37 °C DW. The samples were moved to the next temperature when the shape no longer changed at a given temperature. The shape fixity (R_f) and shape-recovery ratio (R_r) were calculated using eqs 5 and 6:

$$R_f = \frac{\Theta_t}{\Theta_g} \times 100\ (\%) \tag{5}$$

$$R_r = \frac{\Theta_g - \Theta_f}{\Theta_g} \times 100\ (\%) \tag{6}$$

where Θ_g is the given angle after transform; Θ_t is the temporarily fixed angle; and Θ_f is the final angle after recovery at 37 °C.

Cytotoxicity Assays In Vitro. The cytotoxicity of the samples was studied by an extraction test reported in a previous study with a slight modification. NIH/3T3 mouse embryo fibroblast (National Institutes of Health, KCLB21658) which was obtained from the Korean Cell Line Bank (KCLB, Seoul, Korea) was used for this experiment.

The samples were prepared using a biopsy punch, and a total volume of 2.6 mL was obtained. The autoclaved latex was cut into pieces (2.5 cm^2/mL) for the positive control. The prepared samples and latexes were incubated in 10 mL of RPMI (Gibco, USA) supplemented with 10% fetal bovine serum (FBS, Gibco, USA) and 1% penicillin/streptomycin (PS; Gibco, USA) and stored in a 37 °C water bath for 24 h. The extraction solution was filtered through a 0.45 μm pore size filter. The cells were seeded on 96-well plates (n = 6.2 × 10^3 cells/well) in the RPMI cell culture medium and stored in a humidified cell culture incubator (37 °C, 5% CO_2) for 24 h. Then the cell culture medium was replaced with the extracted solution. At specific time points, MTT (3-[4-dimethylathiazol-2-yl]-2,5-diphenyltetrazolium bromide; thiazolyl blue, Amresco, USA) solution was treated and stored under standard culture conditions (at 5% CO_2 and 37 °C) for 3 h. The supernatant was removed, and dimethyl sulfoxide (DMSO; Samchun chemical, South Korea) was added to dissolve the formazan crystal. The absorbance of 570 nm was measured with a microplate reader (Synergy MX, Biotek, Vernusky, VT, USA). All of the groups were normalized with negative control (RPMI medium) and positive control (cell culture medium). Cell viability was calculated using eq 7:

$$\text{cell viability}\ (\%) = \frac{\text{OD}_{\text{sample}}}{\text{OD}_{\text{control}}} \times 100\ (\%) \tag{7}$$

where $\text{OD}_{\text{sample}}$ is the positive control and $\text{OD}_{\text{control}}$ is the negative control.

RESULTS AND DISCUSSION

Structure Confirmation of the Gelatin-Based SMP Scaffolds. The gelatin-based SMP scaffolds were prepared by physically incorporating TA molecules inside the polymer network (Figure 2). Gelatin plays a role in reversibly changing between permanent and temporal shapes in the polymer network. The hydrogen bonding between the carbonyl groups (−C═O) and amide groups (−NH) of gelatin and hydroxyl groups (−OH) of TA serves as reversible net points. As shown in Figure 2A, transparent gelatin-based hydrogels turn into

https://doi.org/10.1021/acsomega.2c06730
ACS Omega 2023, 8, 6455−6462

light-yellow hydrogels after immersion in the TA solution. It was attempted to increase the number of hydrogen bonds between gelatin and TA by adding TA twice in a row. Then the opaque and shrunken hydrogel is formed by soaking in the TA solution, which suggests that triple helix structures of gelatin are destroyed and more hydrogen bonds are formed.

In Gel/OGG/Ca, the double network structure was formed by the physical cross-linking of Ca^{2+} and the chemical cross-linking of OGG. The chemical cross-links were derived from a Schiff base reaction between the amino ($-NH_2$) groups of gelatin and aldehyde ($-CHO$) groups of OGG (Figure 2B). Similarly, several studies have been reported on shape-memory hydrogels through Schiff base reactions.[5,28] Therefore, the combination of gelatin and OGG is expected to provide more stable shape-memory properties.

Chemical Structure Analysis. The chemical composition of tannic acid, gelatin, and oxidized gellan gum and their interactions were analyzed by attenuated total reflectance FT-IR (Figure 3). The spectrum of all materials indicates

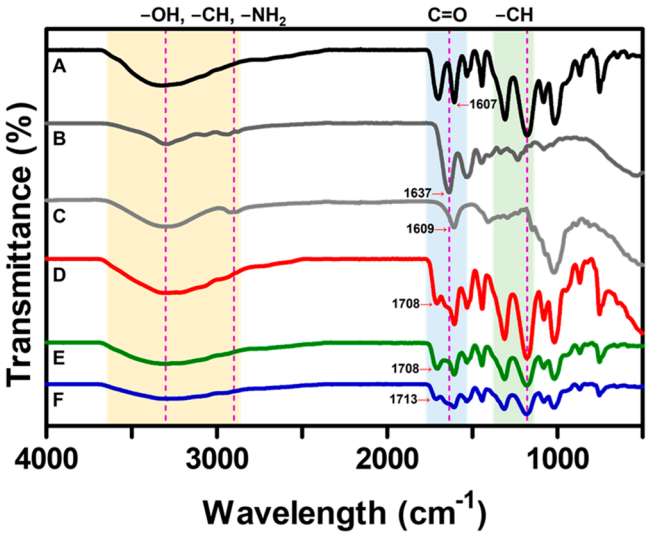

Figure 3. FT-IR analysis of (A) tannic acid, (B) gelatin, (C) oxidized gellan gum, (D) Gel, (E) Gel/Ca, and (F) Gel/OGG/Ca scaffolds in the wavelength range of 400−4000 cm^{-1}.

broadband at 3200−3400 cm^{-1} related to −OH and −NH stretching and a peak at 2800−3000 cm^{-1} associated with −CH stretching. The gelatin and all composites appear overlapping with $-NH_2$ at 3200−3400 cm^{-1}. The −C═O stretching corresponding to the carbonyl group was observed at 1607 cm^{-1} in tannic acid, 1637 cm^{-1} in gelatin, and 1609 cm^{-1} in oxidized gellan gum. The spectra of Gel, Gel/Ca, and Gel/OGG/Ca are similar to that of tannic acid, which suggests that tannic acid has been well bonded to the scaffolds. The peak at 1637 cm^{-1} for the amide I band of gelatin shifts to 1708 cm^{-1} in Gel and Gel/Ca and 1713 cm^{-1} in Gel/OGG/Ca after sample formation, which indicates the occurrence of electrostatic complexation between the gelatin and tannic acid.[29,30] The characteristic peaks were observed corresponding to (out-of-plane) aromatic C−H bending vibrations of tannic acid at 1000−1300 cm^{-1} in the spectrum of scaffolds.[31,32] The Gel/OGG/Ca showed a peak intensity lower than that of Gel/Ca, which is attributed to a covalent interaction between the amide I group of gelatin and aldehyde groups of oxidized gellan gum.

Morphological Observation. FE-SEM was measured to observe the surface texture and morphology of the scaffold. The surface properties of the scaffolds affect not only water and nutrient penetration but also cell adhesion, spreading, and proliferation. The gel shows a smooth surface, whereas relatively rougher surfaces are observed in Gel/Ca and Gel/OGG/Ca after surface functionalization (Figure 4). Because

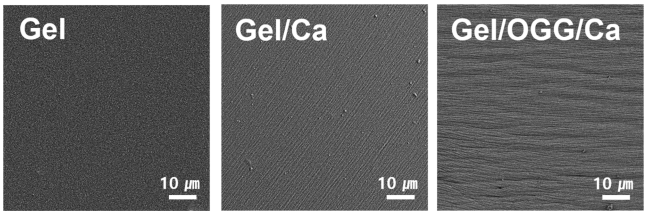

Figure 4. FE-SEM images showing the surface morphology of the scaffolds.

surface roughness can promote the initial cell adhesion,[33] these results suggest that surface functionalization of gelatin with $CaCl_2$ and OGG can improve surface properties.

Physicochemical Analysis. Physicochemical analysis was conducted to test mass swelling, sol fraction, weight loss, and porosity (Figure 5). Overall, four analyses showed a similar tendency. The mass swelling was measured to demonstrate the water absorption of the sample. The swelling capacity plays a critical role in preserving culture media in vitro and the body fluid and nutrients in vivo. The swelling capacity of Gel and Gel/Ca displayed 4.0 ± 0.02 and 4.1 ± 0.1, which means that the ionic bond between gelatin and calcium chloride does not affect the entire matrix (Figure 5A). On the other hand, the Gel/OGG/Ca showed 3.1 ± 0.1, which was a noticeable decrease compared with the two groups in front. This is regarded as a result of the reduced swelling property by cross-linking between Gel and OGG.

The sol fraction shows an uncross-linked polymer fraction. The sol fraction of the scaffolds appears to be 5.2 ± 0.7, 4.4 ± 0.6, and 2.1 ± 0.7% in Gel, Gel/Ca, and Gel/OGG/Ca, respectively (Figure 5B). These results are related to the interaction of the matrix. The lower sol fraction of the Gel/Ca and Gel/OGG/Ca was considered due to the cross-linking density increased by adding $CaCl_2$ and OGG. In other words, the lowest rate of OGG indicates the most binding.

The scaffolds for TE should be gradually degraded for tissue regeneration and completely removed after a certain period of time. To prove this, weight loss was observed for 28 days (Figure 5C). Generally, the rate of degradation is related to the cross-linking density and the molecular weight of polymers. As time passed, weight loss occurred gradually in all groups. The Gel/OGG/Ca group showed the slowest degradation rate. At the end of the experiment, the weight loss was observed to be 39.9 ± 2.3, 32.7 ± 3.5, and 29.3 ± 0.2% in Gel, Gel/Ca, and Gel/OGG/Ca, respectively. Compared with only physically cross-linked scaffolds, Gel/OGG/Ca containing physical and chemical cross-linking mechanisms delayed the degradation rate.

The porosity of the scaffolds affects cell adhesion, penetration, proliferation, and nutrient exchange. The porosity of the scaffolds was 82.5 ± 1.6, 74.0 ± 2, and 63.1 ± 1.3% in Gel, Gel/Ca, and Gel/OGG/Ca, respectively (Figure 5D). All groups showed more than 60% porosity, so it seems to be no problem in cell seeding.

https://doi.org/10.1021/acsomega.2c06730
ACS Omega 2023, 8, 6455−6462

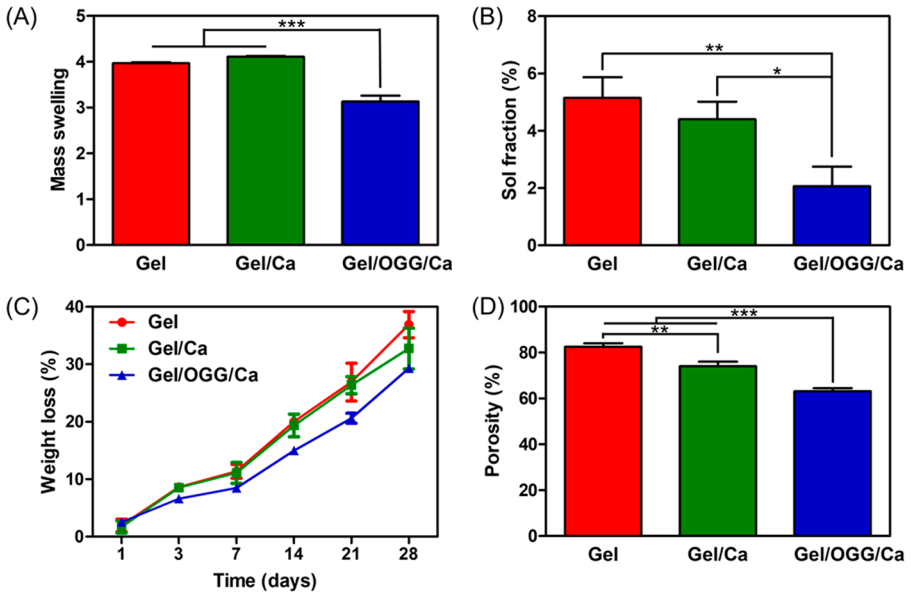

Figure 5. Physicochemical analysis of the scaffolds: (A) mass swelling, (B) sol fraction, (c) weight loss, and (D) porosity (values are mean ± SD, n = 4, $P < 0.05$ (*), $P < 0.01$ (**), and $P < 0.001$ (***)).

Mechanical Analysis. A tensile test was performed to evaluate the mechanical properties of the scaffold. The stress−strain curve is shown in Figure 6. All groups were observed to have increased tensile stress rapidly as deformation increased, and then parts were damaged after reaching the yield point. The Gel has tensile strength of ∼1.94 MPa and elongation of 155%. The Gel/OGG/Ca showed the highest tensile strength (∼2.4 MPa) and elongation (197.5%). Generally, high porosity has a low tensile strength, and Gel and Gel/OGG/Ca show the same results. On the other hand, the Gel/Ca showed the lowest tensile strength (∼0.9 MPa) and elongation (148.4%) because $CaCl_2$ weakened the cohesion of the triple helix in gelatin; therefore, the structure became loose.

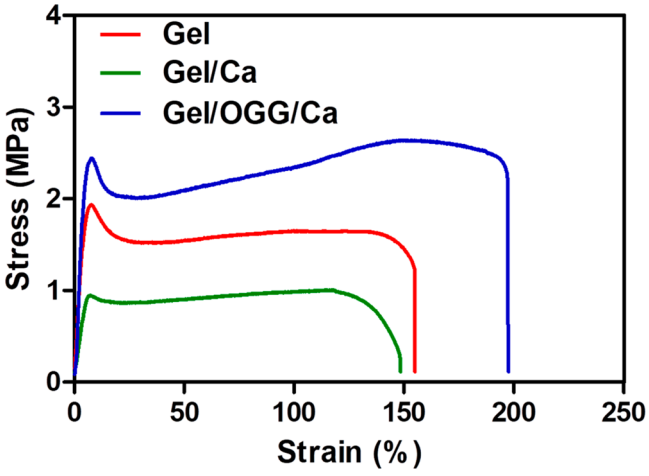

Figure 6. Mechanical characterization of Gel, Gel/Ca, and Cel/OGG/Ca. Tensile stress−strain curves of the scaffolds at a speed of 20 mm/min.

Shape-Memory Behavior. The shape-recovery process was tested at the physiological temperature (37 °C) to identify the potential for use in biomedical applications. Figure 7A shows the shape-memory behavior of the scaffolds, and the recovery of the sample was assessed after being triggered in DW at 37 °C for an equal time (20 s). The Gel/OGG/Ca showed the fastest recovery, which is presumed to be the result of chemical cross-linking between gelatin and OGG. Thus, Gel/OGG/Ca can be regarded as the most suitable scaffold for the application of minimally invasive transplantation compared to other groups. According to Figure 7B, the scaffolds can be softly tied and twisted without cracking, which demonstrates robust mechanical properties and flexibility. To evaluate this in detail, the shape fixity (R_f) and shape recovery (R_r) of the Gel/OGG/Ca were calculated (Figure 7C). The Gel/OGG/Ca displayed a R_f value (97.7%) at 25 °C and a R_r value (95.8%) at 37 °C for approximately 30 s.

In all groups, the temporary shape was restored to the original shape within about 30 s. The results of shape-recovery time and recovery ratio were similar in three repeated tests. These results indicate that the hydrogen bonding and triple helix of the gelatin chains in the scaffolds are sensitively responsive to temperature changes and stable in repeat tests.

Cytotoxicity Assays In Vitro. Cytotoxicity assay on NIH/3T3 cells was performed to evaluate cell compatibility (Figure 8). Cell compatibility is significant in determining whether a material can be used for biomedical applications. Generally, 75% or more of cell viability means that there is no cytotoxicity.[34] All groups except the positive control showed more than 95%, and there were no significant variations between the groups on 1 day of the experiment. However, only the negative control and Gel/OGG/Ca showed more than 75%, which means noncytotoxicity of the scaffold after 2 days of the experiment. Finally, all groups except the negative control showed a result of less than 75% on 3 days of the experiment, for which it is presumed that cell viability has been reduced by a continuous release of tannic acid.[35] As time passed, all scaffolds were gradually cytotoxicy, but Gel/OGG/Ca (68.37 ± 0.04%) had relatively weaker cytotoxicity compared to that of the other groups. These results suggest that Gel/OGG/Ca can suppress the release of tannic acids. Furthermore, the amount of oxidized polysaccharides in OGG seems to be appropriate considering too many aldehyde groups

https://doi.org/10.1021/acsomega.2c06730
ACS Omega 2023, 8, 6455−6462

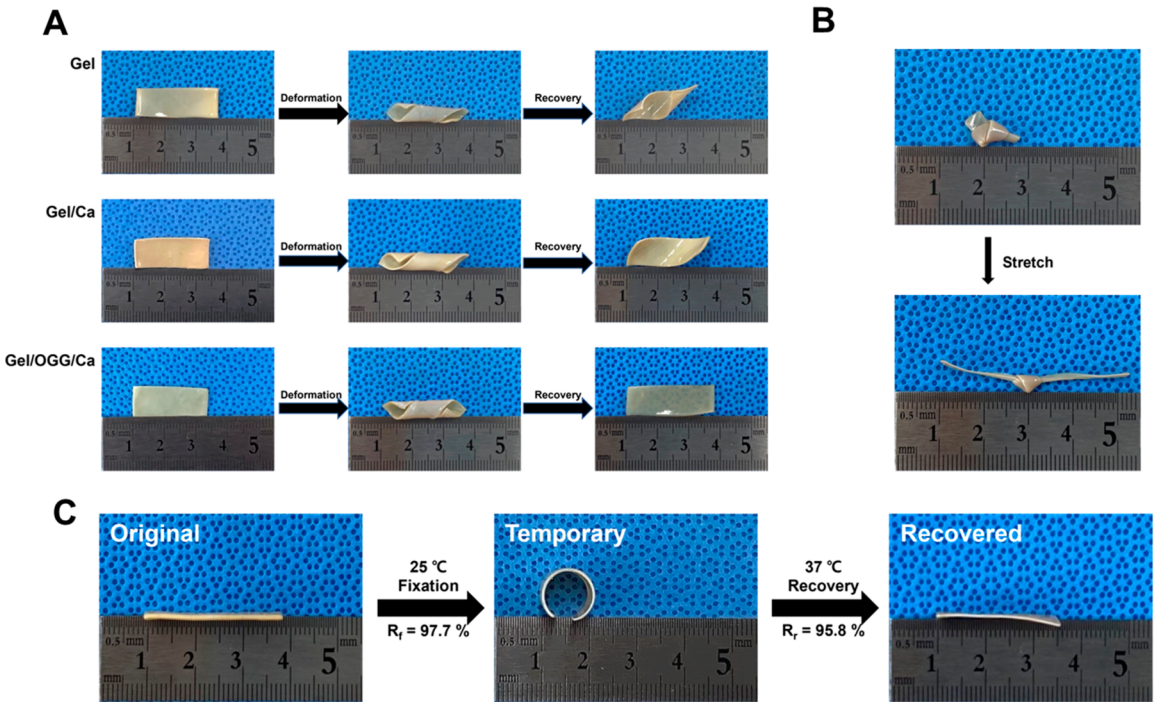

Figure 7. (A) Photographs of physical deformation and recovery of Gel, Gel/Ca, and Gel/OGG/Ca. Photographs of (B) knotted Gel/OGG/Ca and (C) recovered Gel/OGG/Ca at 37 °C.

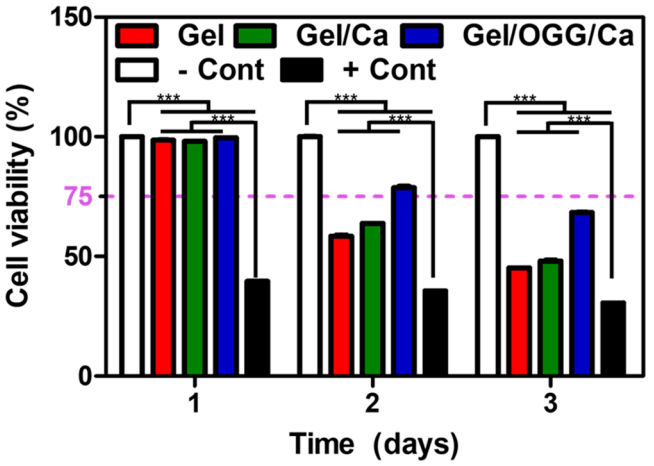

Figure 8. Cytotoxicity of the scaffolds was evaluated on 1, 2, and 3 days (values are mean ± SD, n = 8, P < 0.001 (***)).

can cause cytotoxicity.[36] Overall, Gel/OGG/Ca is regarded to be biocompatible and can be used for further in vitro study.

CONCLUSIONS

In this study, the temperature-responsive-type memory scaffold was successfully developed by immersing it in an aqueous tannic acid solution. Hydrogen bonds between gelatin and tannic acid form memory as a reversible purity. All scaffolds were temporarily fixed at 25 °C in 1 s due to their fast reaction rate and restored to their original form at 37 °C in 30 s. In particular, Gel/OGG/Ca had excellent shape fixation and shape recovery estimated by the introduction of the Shiff base structure. In addition, the proper amount of oxidation did not induce cytotoxicity and improved the mechanical properties of the scaffold and the structural stability of the substrate. Cell viability analysis showed that Gel/OGG/Ca is cell-compatible and may be suitable for further in vitro studies. Further research is needed to confirm the effectiveness and prove its applicability. The strategy proposed in this study suggests that it can be autonomously placed in difficult-to-access places such as the human body and space and that it can be applied to various applications by changing its original shape and changing its temporary shape.

AUTHOR INFORMATION

Corresponding Author

Gilson Khang − *Department of Bionanotechnology and Bio-Convergence Engineering and Department of PolymerNano Science & Technology and Polymer Materials Fusion Research Center, Jeonbuk National University, Jeonju-si, Jeonbuk 54896, Korea; Department of Orthopaedic & Traumatology, Airlangga University, Kota SBY, Jawa Timur 60115, Indonesia;* orcid.org/0000-0002-6452-5653; Email: gskhang@jbnu.ac.kr

Authors

Na Eun Kim − *Department of Bionanotechnology and Bio-Convergence Engineering, Jeonbuk National University, Jeonju-si, Jeonbuk 54896, Korea*

Sunjae Park − *Department of Bionanotechnology and Bio-Convergence Engineering, Jeonbuk National University, Jeonju-si, Jeonbuk 54896, Korea*

Sooin Kim − *Department of Bionanotechnology and Bio-Convergence Engineering, Jeonbuk National University, Jeonju-si, Jeonbuk 54896, Korea*

Joo Hee Choi − *Department of Bionanotechnology and Bio-Convergence Engineering, Jeonbuk National University, Jeonju-si, Jeonbuk 54896, Korea;* orcid.org/0000-0002-6424-1810

Se Eun Kim − *Department of Bionanotechnology and Bio-Convergence Engineering, Jeonbuk National University, Jeonju-si, Jeonbuk 54896, Korea*

https://doi.org/10.1021/acsomega.2c06730
ACS Omega 2023, 8, 6455−6462

Seung Ho Choe − *Department of Bionanotechnology and Bio-Convergence Engineering, Jeonbuk National University, Jeonju-si, Jeonbuk 54896, Korea*

Tae woong Kang − *Department of Bionanotechnology and Bio-Convergence Engineering, Jeonbuk National University, Jeonju-si, Jeonbuk 54896, Korea*

Jeong Eun Song − *Department of Bionanotechnology and Bio-Convergence Engineering, Jeonbuk National University, Jeonju-si, Jeonbuk 54896, Korea;* orcid.org/0000-0001-6879-7616

Complete contact information is available at: https://pubs.acs.org/10.1021/acsomega.2c06730

Author Contributions

N.E.K. and S.P. contributed equally to this work. N.E.K. and S.P. designed and conducted the experiments and wrote the draft of the manuscript. S.K. and J.H.C. conducted the experiments and analyzed the data. S.E.K. and S.H.C. participated in the cell experiments and the SEM imaging. S.P., J.E.S., and T.W.K. supervised the project and polished the manuscript. G.K. proposed the initial idea of this project, supervised the project, and revised the manuscript.

Notes

The authors declare no competing financial interest.

■ ACKNOWLEDGMENTS

This research was supported by the International Research & Development Program of the National Research Foundation of Korea (NRF) funded by the Ministry of Science, ICT & Future Planning (2021K1A3A1A78097905).

■ REFERENCES

(1) Osada, Y.; Matsuda, A. Shape memory in hydrogels. *Nature* **1995**, *376* (6537), 219−219.

(2) Otsuka, K.; Wayman, C. M. *Shape Memory Materials*; Cambridge University Press, 1999.

(3) Wang, J.; Zhao, Q.; Wang, Y.; Zeng, Q.; Wu, T.; Du, X. Self-Unfolding Flexible Microelectrode Arrays Based on Shape Memory Polymers. *Advanced Materials Technologies* **2019**, *4* (11), 1900566.

(4) Montgomery, M.; Ahadian, S.; Davenport Huyer, L.; Lo Rito, M.; Civitarese, R. A.; Vanderlaan, R. D.; Wu, J.; Reis, L. A.; Momen, A.; Akbari, S.; et al. Flexible shape-memory scaffold for minimally invasive delivery of functional tissues. *Nature materials* **2017**, *16* (10), 1038−1046.

(5) Mao, Q.; Hoffmann, O.; Yu, K.; Lu, F.; Lan, G.; Dai, F.; Shang, S.; Xie, R. Self-contracting oxidized starch/gelatin hydrogel for noninvasive wound closure and wound healing. *Materials & Design* **2020**, *194*, 108916.

(6) Zhang, D.; George, O. J.; Petersen, K. M.; Jimenez-Vergara, A. C.; Hahn, M. S.; Grunlan, M. A. A bioactive "self-fitting" shape memory polymer scaffold with potential to treat cranio-maxillo facial bone defects. *Acta biomaterialia* **2014**, *10* (11), 4597−4605.

(7) Baker, R. M.; Tseng, L.-F.; Iannolo, M. T.; Oest, M. E.; Henderson, J. H. Self-deploying shape memory polymer scaffolds for grafting and stabilizing complex bone defects: A mouse femoral segmental defect study. *Biomaterials* **2016**, *76*, 388−398.

(8) Xie, R.; Hu, J.; Hoffmann, O.; Zhang, Y.; Ng, F.; Qin, T.; Guo, X. Self-fitting shape memory polymer foam inducing bone regeneration: A rabbit femoral defect study. *Biochimica et Biophysica Acta (BBA)-General Subjects* **2018**, *1862* (4), 936−945.

(9) Huang, K.; Yang, M.-s.; Tang, Y.-j.; Ling, S.-Y.; Pan, F.; Liu, X.-d.; Chen, J. Porous shape memory scaffold of dextran and hydroxyapatite for minimum invasive implantation for bone tissue engineering applications. *Journal of Biomaterials Applications* **2021**, *35* (7), 823−837.

(10) Wu, X.; Huang, W.; Seow, Z.; Chin, W.; Yang, W.; Sun, K. Two-step shape recovery in heating-responsive shape memory polytetrafluoroethylene and its thermally assisted self-healing. *Smart materials and structures* **2013**, *22* (12), 125023.

(11) Inoue, K.; Yamashiro, M.; Iji, M. Recyclable shape-memory polymer: Poly (lactic acid) crosslinked by a thermoreversible Diels−Alder reaction. *J. Appl. Polym. Sci.* **2009**, *112* (2), 876−885.

(12) Wu, X.; Huang, W.; Tan, H. Characterization of shape recovery via creeping and shape memory effect in ether-vinyl acetate copolymer (EVA). *Journal of Polymer Research* **2013**, *20* (8), 150.

(13) Luo, K.; Wang, L.; Tang, J.; Zeng, X.; Chen, X.; Zhang, P.; Zhou, S.; Li, J.; Zuo, Y. Enhanced biomineralization of shape memory composite scaffolds from citrate functionalized amorphous calcium phosphate for bone repair. *J. Mater. Chem. B* **2021**, *9* (44), 9191−9203.

(14) Chen, Y.-N.; Peng, L.; Liu, T.; Wang, Y.; Shi, S.; Wang, H. Poly (vinyl alcohol)−tannic acid hydrogels with excellent mechanical properties and shape memory behaviors. *ACS Appl. Mater. Interfaces* **2016**, *8* (40), 27199−27206.

(15) Du, L.; Yang, S.; Li, W.; Li, H.; Feng, S.; Zeng, R.; Yu, B.; Xiao, L.; Nie, H.-Y.; Tu, M. Scaffold composed of porous vancomycin-loaded poly (lactide-co-glycolide) microspheres: A controlled-release drug delivery system with shape-memory effect. *Materials Science and Engineering: C* **2017**, *78*, 1172−1178.

(16) Echave, M. C.; Burgo, L. S.; Pedraz, J. L.; Orive, G. Gelatin as biomaterial for tissue engineering. *Current pharmaceutical design* **2017**, *23* (24), 3567−3584.

(17) Hoque, M. S.; Benjakul, S.; Prodpran, T. Effect of heat treatment of film-forming solution on the properties of film from cuttlefish (Sepia pharaonis) skin gelatin. *Journal of Food Engineering* **2010**, *96* (1), 66−73.

(18) Guo, L.; Colby, R. H.; Lusignan, C. P.; Whitesides, T. H. Kinetics of triple helix formation in semidilute gelatin solutions. *Macromolecules* **2003**, *36* (26), 9999−10008.

(19) Cuppo, F.; Venuti, M.; Cesàro, A. Kinetics of gelatin transitions with phase separation: T-jump and step-wise DSC study. *Int. J. Biol. Macromol.* **2001**, *28* (4), 331−341.

(20) Gornall, J.; Terentjev, E. Universal kinetics of helix-coil transition in gelatin. *Phys. Rev. E* **2008**, *77* (3), 031908.

(21) Gorgieva, S.; Kokol, V. Collagen- vs. gelatine-based biomaterials and their biocompatibility: review and perspectives. *Biomaterials applications for nanomedicine* **2011**, *2*, 17−52.

(22) Drury, J. L.; Mooney, D. J. Hydrogels for tissue engineering: scaffold design variables and applications. *Biomaterials* **2003**, *24* (24), 4337−4351.

(23) Song, F.; Li, Z.; Jia, P.; Zhang, M.; Bo, C.; Feng, G.; Hu, L.; Zhou, Y. Tunable "soft and stiff", self-healing, recyclable, thermadapt shape memory biomass polymers based on multiple hydrogen bonds and dynamic imine bonds. *Journal of Materials Chemistry A* **2019**, *7* (21), 13400−13410.

(24) Yang, Y.; Huang, L.; Wu, R.; Fan, W.; Dai, Q.; He, J.; Bai, C. Assembling of reprocessable polybutadiene-based vitrimers with high strength and shape memory via catalyst-free imine-coordinated boroxine. *ACS Appl. Mater. Interfaces* **2020**, *12* (29), 33305−33314.

(25) Zhang, X.; Do, M. D.; Casey, P.; Sulistio, A.; Qiao, G. G.; Lundin, L.; Lillford, P.; Kosaraju, S. Chemical modification of gelatin by a natural phenolic cross-linker, tannic acid. *Journal of agricultural and food chemistry* **2010**, *58* (11), 6809−6815.

(26) Gong, Y.; Wang, C.; Lai, R. C.; Su, K.; Zhang, F.; Wang, D.-a. An improved injectable polysaccharide hydrogel: modified gellan gum for long-term cartilage regeneration in vitro. *J. Mater. Chem.* **2009**, *19* (14), 1968−1977.

(27) Yang, S.; Zhang, Y.; Wang, T.; Sun, W.; Tong, Z. Ultrafast and programmable shape memory hydrogel of gelatin soaked in tannic acid solution. *ACS Appl. Mater. Interfaces* **2020**, *12* (41), 46701−46709.

(28) Zamani Alavijeh, R.; Shokrollahi, P.; Barzin, J. A thermally and water activated shape memory gelatin physical hydrogel, with a gel

point above the physiological temperature, for biomedical applications. *J. Mater. Chem. B* **2017**, *5* (12), 2302−2314.
(29) Nath, J.; Saikia, P. P.; Handique, J.; Gupta, K.; Dolui, S. K. Multifunctional mussel-inspired Gelatin and Tannic acid-based hydrogel with pH-controllable release of vitamin B12. *J. Appl. Polym. Sci.* **2020**, *137* (39), 49193.
(30) Zheng, Y.; Liang, Y.; Zhang, D.; Sun, X.; Liang, L.; Li, J.; Liu, Y.-N. Gelatin-based hydrogels blended with gellan as an injectable wound dressing. *ACS omega* **2018**, *3* (5), 4766−4775.
(31) Gulley-Stahl, H.; Hogan, P. A.; Schmidt, W. L.; Wall, S. J.; Buhrlage, A.; Bullen, H. A. Surface complexation of catechol to metal oxides: an ATR-FTIR, adsorption, and dissolution study. *Environ. Sci. Technol.* **2010**, *44* (11), 4116−4121.
(32) Luo, D.; Zhang, T.; Zhitomirsky, I. Electrophoretic deposition of tannic acid−polypyrrolidone films and composites. *J. Colloid Interface Sci.* **2016**, *469*, 177−183.
(33) Deng, Y.; Liu, X.; Xu, A.; Wang, L.; Luo, Z.; Zheng, Y.; Deng, F.; Wei, J.; Tang, Z.; Wei, S. Effect of surface roughness on osteogenesis in vitro and osseointegration in vivo of carbon fiber-reinforced polyetheretherketone−nanohydroxyapatite composite. *International journal of nanomedicine* **2015**, *10*, 1425.
(34) Wang, L.; Li, M.; Li, X.; Liu, J.; Mao, Y.; Tang, K. A Biomimetic Hybrid Hydrogel Based on the Interactions between Amino Hydroxyapatite and Gelatin/Gellan Gum. *Macromol. Mater. Eng.* **2020**, *305* (9), 2000188.
(35) Halkes, S. B. A.; van den Berg, A. J.; Hoekstra, M. J.; du Pont, J. S.; Kreis, R. W. Transaminase and alkaline phosphatase activity in the serum of burn patients treated with highly purified tannic acid. *Burns* **2002**, *28* (5), 449−453.
(36) Zhao, J.-L.; Fu, T.; Han, Y.; Xu, K.-W. Reinforcing hydroxyapatite/thermosetting epoxy composite with 3-D carbon fiber fabric through RTM processing. *Mater. Lett.* **2004**, *58* (1−2), 163−168.

https://doi.org/10.1021/acsomega.2c06730
ACS Omega 2023, 8, 6455−6462